# Novel Transmission Line Modeling Method for Nonlinear Permeance Network Based Simulation of Induction Machines

Babak Asghari and Venkata Dinavahi

Department of Electrical and Computer Engineering, University of Alberta, Edmonton, AB T6G 2V4, Canada

**This paper studies different iterative solution methods for nonlinear permeance network based machine models. A new transmission line modeling (TLM) algorithm for efficient solution of permeance network models (PNM) of induction machines is proposed. In this method, the TLM algorithm is used to decouple the nonlinear magnetic equations. The decoupled nonlinear equations are then solved by a look-up table method owing to the repetitive nature of equations across the geometry of the machine. It is shown that the proposed method offers significant speed-up compared to the conventional Newton-Raphson method. Simulation results for dynamic and steady-state conditions of a closed rotor slot induction motor are compared with experimental test results as well as finite element analysis to evaluate the performance of the proposed algorithm.**

*Index Terms*—**Induction machine, iterative methods, Newton-Raphson method, permeance network model, transmission line theory.**

## I. Introduction

THE permeance network model (PNM) is efficacious for studying steady-state and transient performance of electrical machines. This method was originally developed in the late 1980s by Ostovic [1] and has gained increasing popularity due to its accuracy and computational efficiency. It has future potential to be used as a standard method for the design of magnetic devices in automated computer-aided design tools [2]. In a PNM, the major flux paths inside a machine are modeled as a series of interconnected lumped permeance elements. Each permeance element is a flux tube similar to an electric resistance representing a current tube. Gauss' and Ampere's laws of electromagnetics are then applied to obtain permeance network equations of the machine. These equations are solvable by conventional electric circuit methods such as loop or nodal analysis.

The PNM formulations for different types of electrical machines have been developed and used in recent years [3]–[10]. In addition to their application in the design of electrical machines, PNMs can also be used to study fault conditions such as stator winding inter-turn short-circuit [11], [12], broken rotor bars and end rings [12]–[15], and air-gap eccentricity [15] in induction machines. Despite the wide application of permeance network models, a detailed study of nonlinear solution techniques for these networks is not yet available. Fixed-point iteration is commonly used in the literature to obtain the nonlinear solution [7], [16], [17]; however, this method usually suffers from slow convergence rate and excessive computation time. Newton-Raphson (N-R) formulation is also proposed in [18] and [19] where convergence problem is reported during the simulation of a saturated synchronous machine. In this paper, various N-R and transmission line modeling (TLM) based iterative techniques for solving nonlinear PNM equations of an induction machine are discussed and compared with each other. It is shown that permeance network structure lends itself to a novel TLM algorithm which results in the fastest computation speed among the different nonlinear solution algorithms.

The paper is organized as follows. Section II gives the background on the permeance network models. N-R and conventional TLM methods to solve the PNM nonlinear equations are described in Section III. Section IV presents the new TLM solution technique. Results obtained from simulation and experiment are presented and compared with each other in Section V, followed by the conclusion in Section VI.

## II. Background

Analytically permeance values for different parts of an electric machine can be obtained according to the following formula:

$$P = \frac{1}{R} = \frac{1}{\int_0^L \frac{dl}{\mu S(l)}} \tag{1}$$

where $P$, $R$, $L$, $\mu$, and $S$ are permeance, reluctance, length, permeability, and cross-section area of an element, respectively. $l$ is the integration variable. In regions of the machine where the magnetic characteristic is nonlinear (e.g., iron core) the value of permeability is defined as a function of flux density. In a rotating machine, air-gap permeance elements are time-dependent and based on the position of the rotor with respect to the stator.

Fig. 1 shows the PNM for a portion of a squirrel cage induction motor (SCIM) in which the main flux paths are modeled as permeance elements. Magnetomotive force (MMF) sources are specified across the geometry of the machine where electric currents flow inside the stator windings or the rotor bars. Stator MMF sources can be obtained by multiplying the current in each phase by the number of turns in the corresponding slot. For a SCIM, rotor MMF sources are equal to rotor bar currents. A similar approach as in [7] is used here to develop the PNM equations for an induction machine. In this approach a qdo transformation is applied to stator variables to remove the mutual leakage inductance between the windings.

Nodal equations of the permeance network can be written as

$$A_1\mathbf{M} + A_2\mathbf{I} = 0 \tag{2}$$

Manuscript received December 03, 2010; revised February 11, 2011; accepted March 04, 2011. Date of publication March 10, 2011; date of current version July 27, 2011. Corresponding author: V. Dinavahi (e-mail: dinavahi@ece.ualberta.ca).

Color versions of one or more of the figures in this paper are available online at http://ieeexplore.ieee.org.

Digital Object Identifier 10.1109/TMAG.2011.2126049

0018-9464/$26.00 © 2011 IEEE

READ ONLY

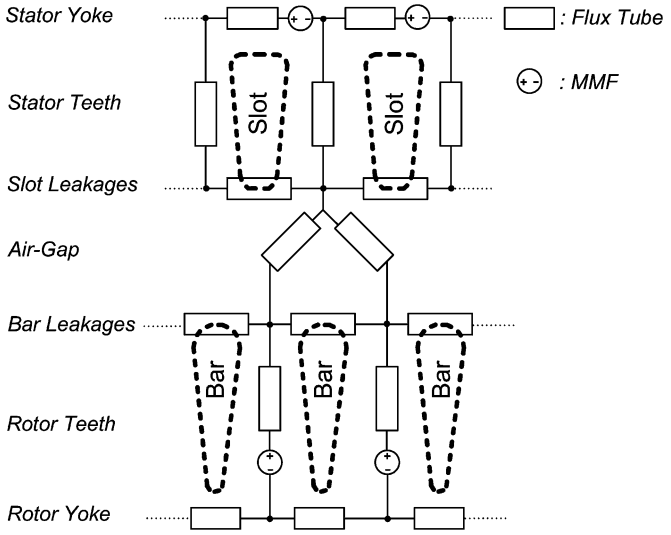


Fig. 1. Permeance network model for a portion of a squirrel cage induction machine.

where $\mathbf{M}$ and $\mathbf{I}$ are vectors of magnetic potentials, and stator phase and rotor bar currents, respectively. $A_1$ is the nodal matrix and $A_2$ includes coefficients of each current in the nodal equations.

Flux linkage equations of stator windings and rotor loops are given as

$$A_3\mathbf{M} + A_4\mathbf{I} = \boldsymbol{\lambda} \tag{3}$$

where $\boldsymbol{\lambda}$ is the vector of stator and rotor flux linkages. $A_3$ and $A_4$ include the contribution of different flux paths of the permeance network into the total flux linkages of stator windings and rotor loops.

Equations (2) and (3) can be combined into a system of nonlinear algebraic equations as follows:

$$A(\boldsymbol{x})\boldsymbol{x} = \boldsymbol{b} \tag{4}$$

where $\boldsymbol{x}$ is the unknown vector including magnetic potentials and stator and rotor bar currents.

Finally, a set of differential equations describe the dynamic behavior of the machine by relating flux linkages and currents to the stator voltage as follows:

$$\frac{d\boldsymbol{\lambda}}{dt} = \begin{bmatrix} \mathbf{v}_{qdo} \\ \mathbf{0} \end{bmatrix} - R\mathbf{I} \tag{5}$$

where $\boldsymbol{\lambda}$, $\mathbf{v}_{qdo}$, and $\mathbf{0}$ are stator and rotor flux linkages, stator voltages (expressed in terms of $qdo$ variables), and short circuit rotor loop voltages, respectively. $R$ is the matrix of stator windings and rotor bars and end rings resistances.

As shown in [20], a special type of sparse linear solver called *Naive* results in the fastest computation time for the linear PNM model. Therefore, the same linear solver is also implemented for the nonlinear model. Different nonlinear solution techniques to solve PNM equations are discussed in the following sections.

## III. Nonlinear Solution of the PNM

The PNM model is used in this section for the transient simulation of a 230 V, 60 Hz, three-phase, four-pole, 5-hp SCIM

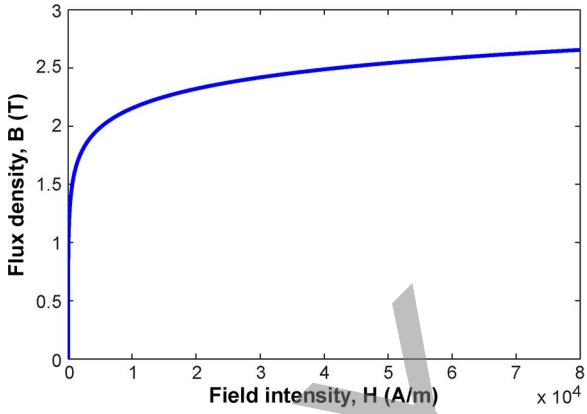


Fig. 2. B-H curve of the core (Machine1).

(Machine1). The motor has 36 stator slots and 28 rotor bars. Detailed parameters of the machine can be found in [7]. The nonlinear B-H characteristic of the core is shown in Fig. 2. The simulation is carried out over a 0.5 s period during the startup of the SCIM under no-load condition with a time-step of $\Delta t = 120\,\mu$s. A step change in the load torque from 0 to 30 N.m occurs at 0.36 s. The system of nonlinear algebraic equations in (4) has a total of 159 unknowns in this case. All simulations are carried out on a Pentium 4 2.8 GHz processor.

### A. N-R Solution

The N-R method is the first algorithm used to solve the nonlinear PNM equations in (4). To apply the N-R algorithm, the nonlinear system of algebraic equations in (4) is rewritten as

$$\boldsymbol{f}(\boldsymbol{x}) = 0. \tag{6}$$

Using the well-known N-R formula, the solution at each iteration is given as

$$\boldsymbol{x}^{k+1} - \boldsymbol{x}^k = -\left(\left[\frac{\partial \boldsymbol{f}^T}{\partial \boldsymbol{x}}\right]^{-1}\right)^k \boldsymbol{f}(\boldsymbol{x}^k) \tag{7}$$

where $\boldsymbol{x}^{k+1}$ and $\boldsymbol{x}^k$ are the solutions at the $(k+1)$-th and $(k)$-th iteration respectively. Matrix $[(\partial \boldsymbol{f}^T/\partial \boldsymbol{x})]$, which is reevaluated at each iteration, is the Jacobian matrix of the system.

The above formula is tested on the PNM with a convergence criteria of

$$\frac{||\boldsymbol{x}^{k+1} - \boldsymbol{x}^k||}{||\boldsymbol{x}^k||} < 10^{-4} \tag{8}$$

and maximum number of iterations limited to 1000. However, convergence problems were observed in multiple time-steps because the knee point of the $B$-$H$ curve is very close to the B-axis. This is a well-known problem in finite element formulation of magnetic scalar potential method [21], [24].

In order to improve convergence, the nonlinear iteration was decelerated by applying an underrelaxation factor $(\alpha)$, as follows:

$$\boldsymbol{x}^{k+1}_{\text{actual}} = \boldsymbol{x}^k + \alpha(\boldsymbol{x}^{k+1} - \boldsymbol{x}^k). \tag{9}$$

In case of using a constant relaxation factor for all iterations, it was found that the value of $(\alpha)$ must be equal to or less than 0.35

READ ONLY

TABLE I
TOTAL SOLUTION TIME FOR DIFFERENT VALUES OF RELAXATION FACTOR (MACHINE1)

| α | Average CPU time (s) |
|---|---|
| 0.35 | 2635 |
| 0.25 | 3980 |
| 0.15 | 6040 |

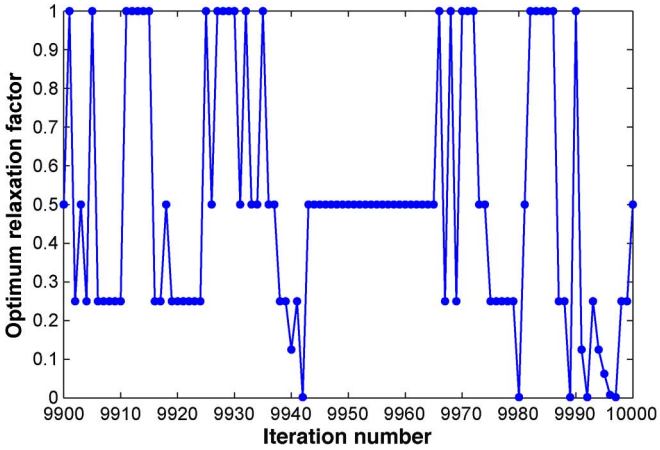


Fig. 3. Optimum relaxation factor at each step of N-R iterations (Machine1).

to obtain convergent results. Table I shows the total simulation time to model 0.5 s of real time for different values of constant $\alpha$. Results suggest that small values of relaxation factor need more iterations and therefore increase the total simulation time for the PNM.

A more efficient way in terms of cpu time and convergence rate is to use an optimized relaxation factor instead of a constant one. In this method, a search procedure is performed within each iteration to find the optimum value of $\alpha$. Several search criteria are proposed in the literature for finite element formulation [21]–[24]. The one used here for the PNM was to choose optimum $\alpha$ in such a way to reduce the $L_2$ norm of residual vector $\boldsymbol{f}$ in each iteration:

$$\|\boldsymbol{f}^{k+1}\| < \|\boldsymbol{f}^{k}\|. \tag{10}$$

The value of the relaxation factor is changed according to the following pattern [23]:

$$\alpha^k = \frac{1}{2^n} \quad (n = 0, 1, \ldots, 10) \tag{11}$$

until the condition in (10) is satisfied or $n$ reaches its maximum value.

Optimized relaxation factor for a portion of transient simulation is depicted in Fig. 3. As can be seen, optimum $\alpha$ varies constantly during the course of simulation. Although the search procedure to obtain optimum $\alpha$ takes some time, it assures convergent results and also reduces total number of N-R iterations. This results in a sharp decline in the total simulation time to 931 s which is only 35% of the total simulation time required for the constant $\alpha$ scheme. Therefore, similar to finite element analysis, the use of an optimized relaxation factor for N-R solution of permeance network models increases the efficiency of simulation considerably.

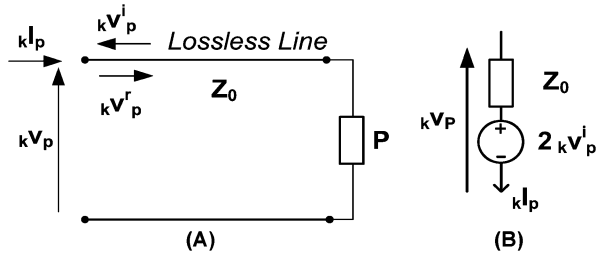


Fig. 4. (a) Nonlinear permeance TLM model. (b) Thévénin equivalent circuit.

### B. TLM Method

The analogy between a PNM and an electrical network allows us to use a different type of nonlinear solution technique known as the transmission line modeling (TLM) method [25] to solve the permeance network equations. In this method, each nonlinear permeance element is connected to the rest of the network through a two-port lossless transmission line, as shown in Fig. 4(a). Substituting the nonlinear permeance elements by their Thévénin equivalent [Fig. 4(b)] in the network, nodal and flux linkage equations of the PNM (2 and 3) must be rewritten based on the new topology and then combined together, as follows:

$$A_{\mathrm{TLM}}\boldsymbol{x} = \boldsymbol{b}_{\mathrm{TLM}}. \tag{12}$$

As can be seen from (12), in the TLM method the coefficient matrix $A_{\mathrm{TLM}}$ is no longer dependent on the vector of unknowns $\boldsymbol{x}$ because the nonlinear permeances in the matrix are replaced by surge impedances of the corresponding transmission lines. In this way, the nonlinearity of system is transferred to the right-hand-side vector $\boldsymbol{b}_{\mathrm{TLM}}$. In a magnetostatic problem, this means that $A_{\mathrm{TLM}}$ is constant and LU decomposition need only be carried out once at the beginning of simulation [26]. In LU decomposition the coefficient matrix is decomposed into the product of a lower triangular matrix $(L)$ and an upper triangular matrix $(U)$ which makes the solution of the linear system quite trivial as it only requires forward and backward substitutions [27]. However, in a PNM of a rotating machine air-gap permeances vary in each time-step based on the position of rotor with respect to the stator. Therefore, $A_{\mathrm{TLM}}$ must be updated and decomposed in each time-step. Nevertheless, as will be shown later, this once per time-step decomposition is still more efficient compared to multiple decompositions within each time-step required in the N-R method.

Considering the $k$th iteration during the $n$th time-step of the transient simulation, the iterative procedure consists of first solving (12) based on the current values of incident waves ${}_kV_p^i$ in $\boldsymbol{b}_{\mathrm{TLM}}$. Having the network solution $(\boldsymbol{x})$, magnetic potentials $({}_kV_p)$ across sending ends of transmission line sections can be obtained from the network topology. The next step is to obtain the reflected wave values $({}_kV_p^r)$ based on transmission line theory as follows:

$${}_kV_p^r = {}_kV_p - {}_kV_p^i. \tag{13}$$

Reflected waves travel toward the receiving end of transmission lines where the nonlinear equation of permeance elements must be satisfied. In a PNM magnetic potential and flux are

READ ONLY

TABLE II
EXECUTION TIME FOR THE N-R AND CONVENTIONAL TLM METHODS (MACHINE1)

| Task | N-R | | TLM | |
|---|---|---|---|---|
| | Execution Time(s) | Execution Time(%) | Execution Time(s) | Execution Time(%) |
| LU Decomposition of $A_{TLM}$ | 578.1 | 62.1 | 6.0 | 5.6 |
| Forward/Backward Substitution | 45.1 | 4.8 | 32.9 | 30.8 |
| N-R Solution for Local Equations | - | - | 58.9 | 55.1 |
| Assembling the Jacobian Matrix | 103.7 | 11.1 | - | - |
| $\alpha$ Optimization | 130.8 | 14.1 | - | - |
| Others | 73.3 | 7.9 | 9.2 | 8.5 |
| Total | 931 | 100 | 107 | 100 |

equivalent to voltage and current in an electric circuit, respectively. Therefore, using transmission line theory the nonlinear equation of a permeance element is given as

$$ {}_kV_p^r - \frac{{}_{k+1}V_p^i}{Z_0} = f_p\left({}_kV_p^r + {}_{k+1}V_p^i\right). \tag{14}$$

Equation (14) is an independent one-dimensional nonlinear equation which can be solved by a scalar N-R method or other methods to obtain the new incident wave $({}_{k+1}V_p^i)$ for each element separately. Having the new incident waves, the iterative procedure proceeds to the next iteration and the same steps are repeated until the desired global convergence criteria (8) is achieved. Then the simulation continues to the next time-step.

To reduce the number of iterations in a nonlinear transient simulation, it is common to use the information from the previous time-step $(n)$ as an initial guess for the new time-step $(n+1)$. In the N-R method this can be done directly by using the final solution from the previous time-step $({}_n\boldsymbol{x})$ as the initial guess in (7). For the TLM method this is not applicable because the previous value of unknown vector $(\boldsymbol{x})$ is not directly involved in the iteration procedure. Two alternate approaches have been tested here. In the first approach, the matrix $A_{\mathrm{TLM}}$ is kept constant during the simulation (except for the change in air-gap permeances) but incident waves from the previous time-step are used as the initial incident waves in the new time-step. In the second approach, in addition to air-gap permeance values, the characteristic impedances of transmission lines are also updated at the beginning of each time-step. The new value of each impedance equals the nonlinear permeance value calculated from the solution in the previous time-step. According to transmission line theory, if the characteristic impedance of each line section is close to the value of its corresponding nonlinear permeance, then fewer global iterations are required to find the network solution. Simulation results show that the first approach is convergent for all time-steps but the results are not accurate. It can be concluded that the incident waves from the previous time-step do not carry valuable information to be used for the initialization in the new time-step. The second approach is also convergent for all time-steps but generates results which match closely with those of the N-R method. Furthermore, by using the TLM method the total computation time to model 0.5 s of real time is reduced to 107 s compared to 931 s for the N-R method.

## IV. LOOK-UP TABLE BASED TLM (LUT-TLM) ALGORITHM

Detailed breakdowns of the total simulation time required in the N-R and conventional TLM methods are shown in Table II. As can be seen from Table II, more than half of the simulation time in the TLM method is spent to solve local one-dimensional nonlinear equations (14) by the use of N-R method. This is due to the large number of nonlinear elements in the PNM. For each nonlinear element a separate N-R solution must be obtained. Therefore, to further decrease the simulation time the solution time for local equations should be shortened.

According to transmission line theory, in an electric circuit (14) describes the relationship between the current (left-hand side) and the voltage $({}_kV_p^r + {}_{k+1}V_p^i)$ at the receiving-end of a transmission line section. In the case of a PNM this is equivalent to the relationship between the magnetic flux flowing through and the magnetic scalar potential across a nonlinear permeance element. Therefore, function $f_p$ can be written as the permeance value times the magnetic scalar potential across an element, i.e.,

$$f_p\left({}_kV_p^r + {}_{k+1}V_p^i\right) = P\left({}_kV_p^r + {}_{k+1}V_p^i\right)\cdot\left({}_kV_p^r + {}_{k+1}V_p^i\right) \tag{15}$$

where $P$ is the nonlinear permeance value described as a function of the magnetic scalar potential.

Based on (15), the local nonlinear equation of (14) for a permeance element can be written as

$$\frac{{}_kV_p^r - {}_{k+1}V_p^i}{Z_0} = P\left({}_kV_p^r + {}_{k+1}V_p^i\right)\cdot\left({}_kV_p^r + {}_{k+1}V_p^i\right). \tag{16}$$

According to (1) it can be observed that function $P$ is dependent on the geometry of a permeance element and the $B$-$H$ characteristic of the magnetic material. Thus, by assuming a similar $B$-$H$ curve for all parts of the machine core, (16) might be different for each nonlinear permeance element depending on its geometry and the value of $Z_0$. Normally in an electrical machine the shapes of stator teeth are identical. This means that for an induction machine with $n_s$ stator slots (teeth) a single nonlinear equation (16) must be solved $n_s$ times with different values of

READ ONLY

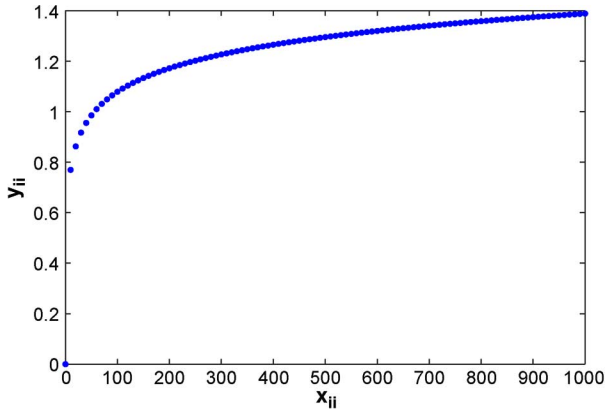


Fig. 5. Look-up table data for stator tooth permeances (Machine1).

${}_kV_p^r$ and $Z_0$ to obtain the new incident waves $({}_{k+1}V_p^i)$ arising from the stator teeth element to be used in the next global iteration. The same argument holds true for other parts of the core such as rotor teeth, and stator and rotor yokes since in a PNM the yoke is divided into identical permeance elements. Therefore, by using the TLM method all decoupled equations of a PNM can be divided into a smaller set of distinct nonlinear equations equal to the number of different shapes available in the permeance network.

The repetitive pattern of the decoupled nonlinear equations in the TLM algorithm suggests that it might be possible to obtain local solutions faster by using look-up tables (LUT-TLM method). In this method for each group of similar nonlinear equations a single look-up table is generated by defining a reference characteristic impedance $Z_0^{ref}$ and two auxiliary variables ($x_{ii}$ and $y_{ii}$) which are given as

$$\begin{aligned} x_{ii} &= \left({}_kV_p^r + {}_{k+1}V_p^i\right), \\ y_{ii} &= \left({}_kV_p^r - {}_{k+1}V_p^i\right). \end{aligned} \tag{17}$$

The relationship between $x_{ii}$ and $y_{ii}$ is set to be

$$y_{ii} = Z_0^{ref} \cdot P(x_{ii}) \cdot x_{ii}. \tag{18}$$

Each look-up table includes several pairs of $x_{ii}$ and $y_{ii}$ obtained from (18) to cover the whole range of changes in the magnetic state of permeance elements with identical geometries. These pairs of data can be generated with any desired resolution and without the need to solve any nonlinear equation. An arbitrary but constant value of $Z_0^{ref}$ is also used in order to normalize the equations. For the SCIM used in this section (Machine1) only permeances related to stator and rotor teeth and stator yoke are considered nonlinear. Therefore only three look-up tables are saved each including 100 pairs of data. Fig. 5 depicts the look-up table data points ($x_{ii}$ and $y_{ii}$) for stator tooth permeance elements of the induction machine. As can be seen the general shape of the look-up data is similar to the $B$-$H$ curve of the core. Due to the symmetry of the $B$-$H$ curve recording of only positive values in the table is sufficient.

By calculating these look-up tables before the start of the simulation, finding local nonlinear solutions during the transient simulation becomes easier and only includes a simple one-dimensional search algorithm. Suppose that for a sample nonlinear permeance element during a global iteration ${}_kV_p^r$ and $Z_0$

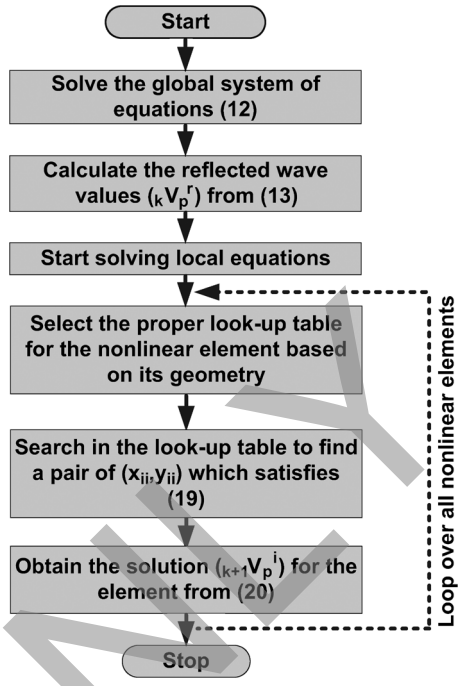


Fig. 6. Flowchart of the LUT-TLM method for a single global iteration.

are known. To obtain ${}_{k+1}V_p^i$, in the first step the corresponding pair of $(x_{ii}, y_{ii})$ should be identified from the proper look-up table. For this purpose based on (16)–(18) ${}_kV_p^r$ is compared with each pair of $(x_{ii}, y_{ii})$ in the table to find a pair which satisfies the following condition:

$$\left|{}_kV_p^r\right| = 0.5 \cdot \left(x_{ii} + \frac{Z_0}{Z_0^{ref}} y_{ii}\right). \tag{19}$$

Once this pair is identified, the value of ${}_{k+1}V_p^i$ is calculated as follows:

$${}_{k+1}V_p^i = sign\left({}_kV_p^r\right) \cdot 0.5 \cdot \left(x_{ii} - \frac{Z_0}{Z_0^{ref}} y_{ii}\right) \tag{20}$$

where the $sign$ function is used to consider both positive and negative values of ${}_kV_p^r$.

Since each look-up table only contains a limited number of data points, usually it is not possible to satisfy (19) exactly. Therefore the pair which results in the closest value to $\left|{}_kV_p^r\right|$ in (19) should be selected. More accurate solutions can also be obtained by using interpolation techniques between neighboring points in the look-up table. However, as mentioned in [28] and also verified for the PNM the tolerance for local equations in the TLM method can be set considerably higher than that of the global equations. Therefore a look-up table with moderate resolution is able to provide accurate results without the need for interpolation. The flowchart of the LUT-TLM method for a single global iteration is given in Fig. 6.

One important advantage of this method is that it eliminates the necessity of defining a monotonic differentiable analytical function for the $B$-$H$ characteristic of iron core similar to the N-R method. Since the real-life measurements of $B$-$H$ data are at discrete points, different methods are proposed to derive such functions [29]. In the look-up table method only discrete points

READ ONLY

TABLE III
EXECUTION TIME FOR THE LUT-TLM METHOD (MACHINE1)

| Task | Execution Time(s) | Execution Time(%) |
|---|---|---|
| LU Decomposition of $A_{TLM}$ | 5.7 | 12.4 |
| Forward/Backward Substitution | 26.7 | 58.0 |
| N-R Solution For Local Equations | 7.9 | 17.2 |
| Others | 5.7 | 12.4 |
| Total | 46 | 100 |

are required which can be obtained directly from measurements. If the number of measurements are insufficient, more intermediate points can be generated by interpolation. Nevertheless, once the look-up table is created with enough resolution, no definition of an analytical function is necessary. The algorithm to convert a $B$-$H$ curve data point $(B_1, H_1)$ to a look-up table data point $(x_{ii}, y_{ii})$ proceeds as follows:

1) Calculate the permeability $(\mu_1)$ as

$$\mu_1 = \frac{B_1}{H_1}. \tag{21}$$

2) Use the geometrical data of the permeance element and the permeability obtained in Step 1 to calculate its permeance value $(P_1)$ from (1).
3) Assuming a constant magnetic field intensity $(H)$ in the permeance element, magnetic scalar potential across the element $(x_{ii})$ is given as

$$x_{ii} = H_1 \cdot L \tag{22}$$

where $L$ is the length of permeance element.
4) Finally, based on (18) calculate the corresponding $(y_{ii})$ as follows:

$$y_{ii} = Z_0^{ref} \cdot P_1 \cdot x_{ii}. \tag{23}$$

The LUT-TLM method was used for the simulation of PNM with the same global convergence criteria as in (8). It was observed that the total simulation time to model 0.5 s of real time decreased to 46 s which is more than 50% reduction in the computation time compared to the conventional TLM method. This is mainly due to the short solution time for the local nonlinear equations in the new look-up table method. Table III shows the breakdown of the total simulation time for the LUT-TLM method.

In this paper a simple sequential search is used to find a data pair in the look-up table since the number of elements in each table is not very large. For tables with more elements it would be more efficient in terms of computation time to use a faster algorithm such as the binary search method.

The decoupling property of the TLM method and repetitive pattern of nonlinearity in a PNM played an important role in the development of the LUT-TLM algorithm. In fact, the proposed method can be used for the solution of any nonlinear system where many elements with similar nonlinear characteristic exist. However, by saving look-up tables the memory efficiency of the algorithm is sacrificed in favor of increasing the computation speed. It is dependent on the specific application to contemplate the overall efficiency of the LUT-TLM algorithm.

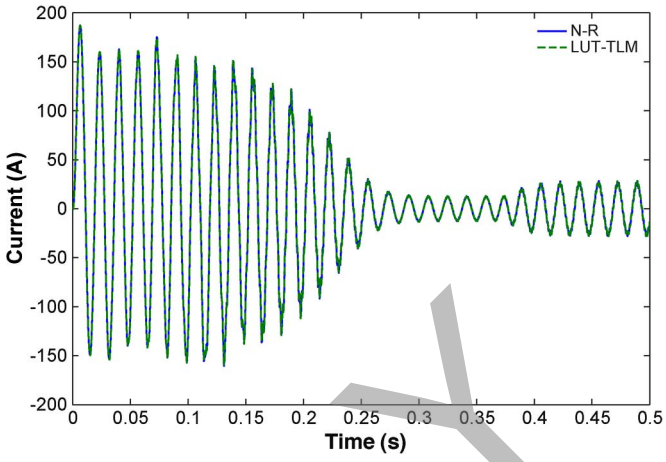


Fig. 7. Simulation results for the stator current. LUT-TLM algorithm versus the N-R method (Machine1).

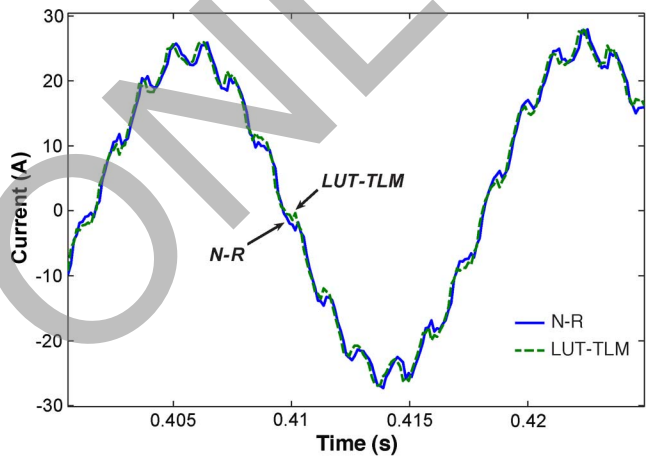


Fig. 8. Simulation results for the steady-state load current. LUT-TLM algorithm versus the N-R method (Machine1).

### A. Time-Domain Simulation Results

In order to examine the accuracy of the LUT-TLM method, its time-domain simulation results are compared with those of the N-R method for Machine1. Since a common time-step and convergence criteria are used for both methods an objective comparison can be achieved. Fig. 7 shows the stator phase A current during the transient and steady-state conditions. A cycle of the same results during loaded condition is also depicted in Fig. 8. Simulation results for the developed electromechanical torque are also presented in Fig. 9. As can be seen the solutions agree reasonably well for the whole period of simulation. Table IV lists the main variables of the machine1 obtained from the use of each method. It was found that the maximum error between the results of two methods is less than 2% for all variables.

## V. EXPERIMENTAL RESULTS

To further evaluate the accuracy of the PNM and LUT-TLM algorithm, several studies were conducted on a 230 V, 60 Hz, three-phase, four-pole, 3-hp SCIM with closed rotor slots (Machine2). Motor data is shown in Table V. The induction motor is mechanically coupled to a DC generator which can be used to load the SCIM. The entire experimental setup is shown in Fig. 10. In closed rotor slot machines, rotor slot bridges have a small radial thickness and are prone to saturation due to the

READ ONLY

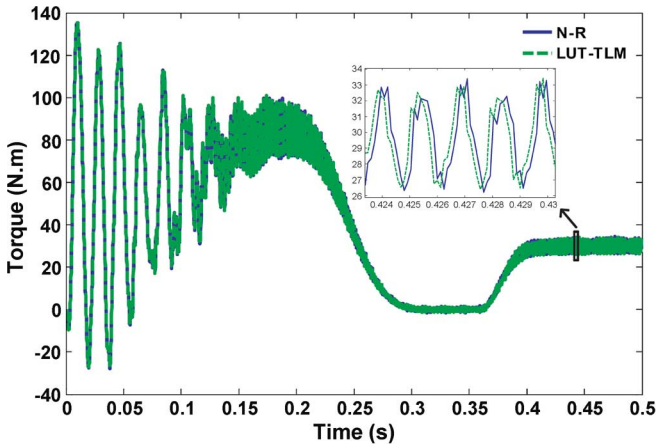


Fig. 9. Simulation results for the electromechanical torque. LUT-TLM algorithm versus the N-R method (Machine1).

TABLE IV
SIMULATION RESULTS FOR THE LUT-TLM AND N-R METHODS (MACHINE1)

| Parameter | N-R | LUT-TLM |
|---|---|---|
| Loaded Speed (rpm) | 1729.3 | 1729.3 |
| Peak Inrush Current (A) | 187.10 | 187.16 |
| Maximum Developed Torque (N.m) | 135.3 | 135.1 |
| Peak No-Load Current (A) | 12.93 | 12.80 |
| Peak Load Current (A) | 28.2 | 28.5 |

TABLE V
TEST MOTOR DATA (MACHINE2)

| Parameter | Value |
|---|---|
| Length (mm) | 107.95 |
| Stator Slots | 36 |
| Stator Outer Diameter (mm) | 195.38 |
| Stator Inner Diameter (mm) | 115.54 |
| Rotor Slots | 28 |
| Average Air-gap Length (mm) | 0.31 |
| Shaft Diameter (mm) | 36.5 |
| Winding Connection | Wye |

currents flowing inside the rotor bars [30]. Thus, in the PNM, in addition to stator and rotor teeth and stator yoke, rotor tooth tip regions should also be modeled with nonlinear permeance elements. This can be easily implemented in the LUT-TLM method by creating a look-up table for these elements as previously described. Therefore, a total of 4 look-up tables are used to model different shapes of nonlinear elements in the PNM of Machine2.

### A. Transient Results

To verify the performance of the proposed method during the transient operation of an induction machine, a simulation were carried out to predict the inrush current when the test motor (Machine2) was started directly from a 208 V three-phase supply under no-load conditions. During the test a current probe was used to capture the inrush current waveform on the oscilloscope. This waveform was then downloaded onto a PC and plotted as shown in Fig. 11(a). The PNM simulation results obtained under the same conditions by using the LUT-TLM algorithm are also

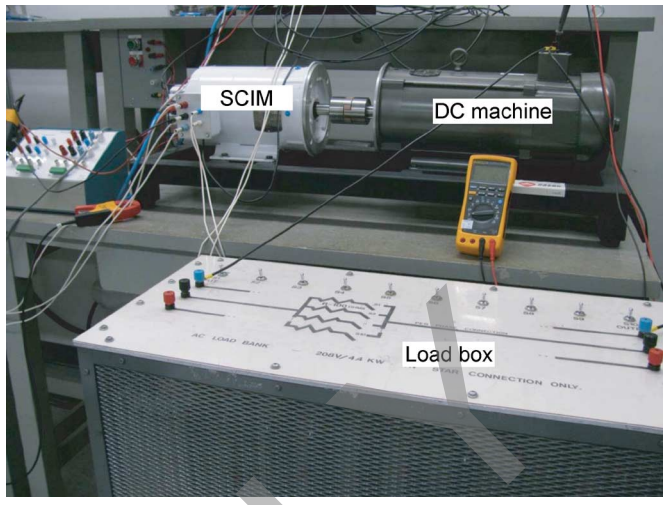


Fig. 10. Experimental setup for Machine2.

depicted in Fig. 11(b). It can be seen that the simulated inrush current is in good agreement with the measurement. The peak current predicted by the PNM is 90.5 A while the measured peak current is 102.2 A. Both currents decay over approximately 0.4 s. The total LUT-TLM simulation time required for modeling 0.5 s of real time was slightly higher for machine2 compared to machine1 (52 s). This is due to the fact that Machine2 has more nonlinear permeance elements because of its closed rotor slots. Nevertheless, the LUT-TLM method still results in a lower simulation time compared to the conventional TLM and N-R methods.

### B. Steady-State Results

In this study Machine2 was simulated at steady-state operating points with different rotational speeds. The results obtained from the PNM with LUT-TLM algorithm and a 2-D finite element analysis (FEA) using the JMAG software are compared with the actual measurements. Fig. 12 shows the simulated and measured steady-state torque values for this machine. It can be seen that both PNM and FEA predict the developed torque with a good accuracy (within 10% error) except for the speeds very close to the synchronous speed. The discrepancy of the results can be attributed in part to neglecting the core loss in both PNM and FEA. As the core loss is the main loss component around the synchronous speed the lack of a detailed loss model can deteriorate the simulation results. Also, since the developed torque around the synchronous speed is small the accuracy of measurements is slightly lower. Another observation from the torque plot is that the PNM tends to overestimate the torque value at larger speeds and underestimate it for smaller speeds while the torque obtained from FEA is slightly larger than the measurement for all speeds. This is mainly due to the fact that the method of torque calculation in the PNM (average torque value) is different than that of the FEA (nodal force method). The results obtained from the simulation and measurements for the steady-state stator current are shown in Fig. 13. In this case the difference between the simulation results and measurements is less than 10% for all operating points. The simulated stator current is always slightly lower compared to the measured one due to the lack of core loss modeling in the simulation. Other

READ ONLY

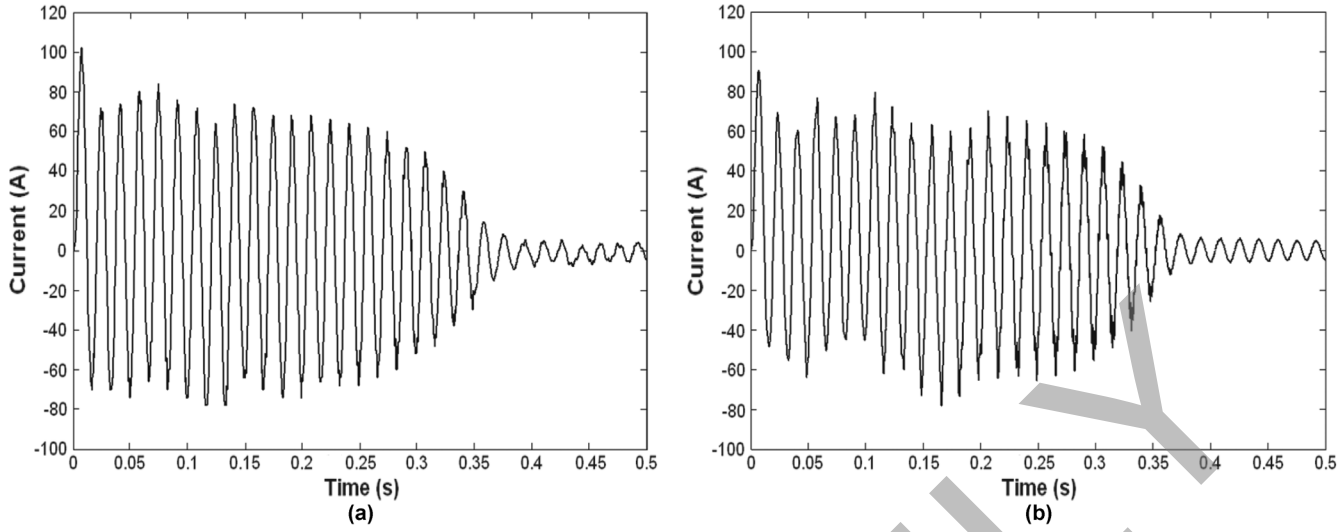


Fig. 11. Stator phase-a inrush current (Machine2): (a) experimental results; (b) simulation results (LUT-TLM method).

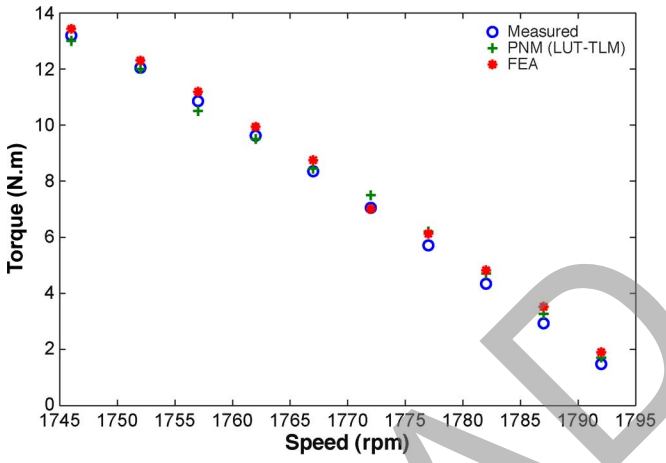


Fig. 12. Comparison of steady-state torque values for Machine2.

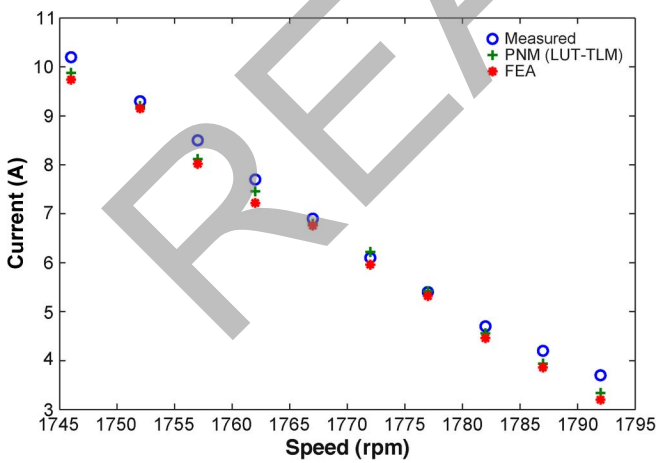


Fig. 13. Comparison of steady-state stator currents for Machine2.

reasons for the discrepancies observed in the results are approximating the cylindrical structure of the induction machine by cuboid permeance elements, neglecting the skew effect in rotor bars, and using an ideal sinusoidal voltage source in the simulation models while the voltage source in the experiment was slightly distorted.

Overall, it was concluded that both PNM and FEA provide acceptable simulation results in comparison with the measurement for a closed rotor slot machine. However, from a computational perspective the PNM with LUT-TLM algorithm provides considerable advantages over the FEA. It was found that the computation time for simulation of a single steady-state cycle using FEA is around 1800 s while the same simulation only takes 1.7 s to be completed for the PNM with the LUT-TLM algorithm.

## VI. Conclusion

This paper provides a comprehensive study of two main nonlinear solution methods, namely N-R and TLM techniques for the simulation of permeance network models (PNM) of induction machines. It has been shown that similar to finite element analysis the use of an optimized relaxation factor in the iterations can improve convergence and decrease the simulation time for the N-R method. The simulation results also suggest that the use of TLM method with updated characteristic impedances at the beginning of each time-step can offer considerable reduction in simulation time compared to the N-R method. In order to speed up the simulation further, a new TLM algorithm (LUT-TLM) is proposed based on the use of look-up tables for the solution of the decoupled nonlinear equations. Comparison between time-domain simulation results of the LUT-TLM algorithm and the N-R method shows that the results are in close agreement during steady-state and transient operations. The LUT-TLM method is then used for the simulation of a closed rotor slot induction machine and the results are verified against FEA and measurements. The proposed LUT-TLM algorithm is a good candidate for real-time simulation of electric machines which places stringent constraints on model execution time while demanding high accuracy. Such real-time models can then be used in hardware-in-the-loop (HIL) simulations to test new controllers and power electronics modules against accurate virtual models of electric machines. The proposed algorithm can also be used in the simulation of other nonlinear systems where multiple elements with similar nonlinear characteristics are present.

READ ONLY

## ACKNOWLEDGMENT

This work was supported by the Natural Sciences and Engineering Research Council of Canada (NSERC).

## REFERENCES

[1] V. Ostovic, "A novel method for evaluation of transient states in saturated electric machines," *IEEE Trans. Ind. Appl.*, vol. 25, no. 1, pp. 96–100, Jan.–Feb. 1989.

[2] A. Delale, L. Albert, L. Gerbaud, and F. Wurtz, "Automatic generation of sizing models for the optimization of electromagnetic devices using reluctance networks," *IEEE Trans. Magn.*, vol. 40, no. 2, pp. 830–833, Mar. 2004.

[3] C. Delforge and B. Lemaire-Semail, "Induction machine modeling using finite element and permeance network methods," *IEEE Trans. Magn.*, vol. 31, no. 3, pp. 2092–2095, May 1995.

[4] M. Hecquet and P. Brochet, "Modeling of a claw-pole alternator using permeance network coupled with electric circuits," *IEEE Trans. Magn.*, vol. 31, no. 3, pp. 2131–2134, May 1995.

[5] J. Farooq, S. Srairi, A. Djerdir, and A. Miraoui, "Use of permenace network method in the demagnetization phenomenon modeling in a permanent magnet motor," *IEEE Trans. Magn.*, vol. 42, no. 4, pp. 1295–1298, Apr. 2006.

[6] D. Petrichenko, M. Hecquet, P. Brochet, V. Kuznetsov, and D. Laloy, "Design and simulation of turbo-alternator using a coupled permeance network model," *IEEE Trans. Magn.*, vol. 42, no. 42, pp. 1259–1262, April 2006.

[7] S. D. Sudhoff, B. T. Kuhn, K. A. Corzine, and B. T. Branecky, "Magnetic equivalent circuit modeling of induction motors," *IEEE Trans. Energy Convers.*, vol. 22, no. 2, pp. 259–270, Jun. 2007.

[8] Y. Chen and Z. Q. Zhue, "Three-dimensional lumped-parameter magnetic circuit analysis of single-phase flux-switching permanent-magnet motor," *IEEE Trans. Ind. Appl.*, vol. 44, no. 6, pp. 1701–1710, Nov./Dec. 2008.

[9] S.-H. Mao, D. Dorrell, and M.-C. Tsai, "Fast analytical determination of aligned and unaligned flux linkage in switched reluctance motors based on a magnetic circuit model," *IEEE Trans. Magn.*, vol. 45, no. 7, pp. 2935–2942, Jul. 2009.

[10] S.-H. Lee, S.-O. Kwon, J.-J. Lee, and J.-P. Hong, "Characteristic analysis of claw-pole machine using improved equivalent magnetic circuit," *IEEE Trans. Magn.*, vol. 45, no. 10, pp. 4570–4573, Oct. 2009.

[11] A. Mahyob, M. Elmoctar, P. Reghem, and G. Barakat, "Coupled magnetic circuit method and permeance network method modeling of stator faults in induction machines," in *Proc. IEEE 13th Conf. Power Electronics and Motion Control*, Sep. 2008, pp. 810–817.

[12] G. Y. Sizov, C.-C. Yeh, and N. A. O. Demerdash, "Magnetic equivalent circuit modeling of induction machines under stator and rotor fault conditions," in *Proc. IEEE Int. Conf. Elec. Machines and Drives*, May 2009, pp. 119–124.

[13] M. Derrhi, C. Delmotte-Delforge, and P. Brochet, "Fault simulation of induction machines using a coupled permeance network model," in *Proc. IEEE Int. Symp. Diagnostics for Electrical Machines, Power Electronics and Drives*, Sep. 1999, pp. 401–406.

[14] C. Delmotte-Delforge, H. Henao, G. Ekwe, P. Brochet, and G.-A. Capolino, "Comparison of two modeling methods for induction machine study: Application to diagnosis," *COMPEL: Int. J. Comput. Math. Elect. Electron. Eng.*, vol. 22, no. 4, pp. 891–908, 2003.

[15] A. Mahyob, M. Y. O. Elmoctar, P. Reghem, and G. Barakat, "Induction machine modelling using permeance network method for dynamic simulation of air-gap eccentricity," in *Proc. 12th Eur. Conf. Power Electronics and Applications*, Sep. 2007, pp. 1–9.

[16] M. A. Batdorff and J. H. Lumkes, "High-fidelity magnetic equivalent circuit model for an axisymmetric electromagnetic actuator," *IEEE Trans. Magn.*, vol. 45, no. 8, pp. 3064–3072, Aug. 2009.

[17] B. Sheikh-Ghalavand, S. Vaez-Zadeh, and A. H. Isfahani, "An improved magnetic equivalent circuit model for iron-core linear permanent-magnet synchronous motors," *IEEE Trans. Magn.*, vol. 46, no. 1, pp. 112–120, Jan. 2010.

[18] M. Amrhein and P. T. Krein, "3-D magnetic equivalent circuit framework for modeling electromechanical devices," *IEEE Trans. Energy Convers.*, vol. 24, no. 2, pp. 397–405, Jun. 2009.

[19] M. L. Bash, J. M. Williams, and S. D. Pekarek, "Incorporating motion in mesh-based magnetic equivalent circuits," *IEEE Trans. Energy Convers.*, pp. 1–10, 2010.

[20] B. Asghari and V. Dinavahi, "Permeance network based real-time induction machine model," in *Int. Power System Transients Conf. (IPST 2009)*, Kyoto, Jun. 2009, pp. 1–6.

[21] T. Nakata, N. Takahashi, K. Fujiwara, N. Okamoto, and K. Muramatsu, "Improvement of convergence characteristics of Newton-Raphson method for nonlinear magnetic field analysis," *IEEE Trans. Magn.*, vol. 28, no. 2, pp. 1048–1051, Mar. 1992.

[22] R. Albanese and G. Rubinacci, "Numerical prosedure for the solution of nonlinear electromagnetic problems," *IEEE Trans. Magn.*, vol. 28, no. 2, pp. 1228–1231, Mar. 1992.

[23] K. Fujiwara, T. Nakata, N. Okamoto, and K. Muramatsu, "Method for determining relaxation factor for modified Newton-Raphson method," *IEEE Trans. Magn.*, vol. 29, no. 2, pp. 1962–1965, Mar. 1993.

[24] C. Neagoe and F. Ossart, "Analysis of convergence in nonlinear magnetostatic finite elements problems," *IEEE Trans. Magn.*, vol. 30, no. 5, pp. 2865–2868, Sep. 1994.

[25] P. B. Johns and M. O'Brien, "Use of transmission-line method to solve nonlinear lumped networks," *Radio Electron. Eng.*, vol. 50, no. 1/2, pp. 59–70, Jan. 1980.

[26] J. Lobry, J. Trecat, and C. Broche, "The transmission line modeling method as a new iterative technique in nonlinear magnetostatics," *IEEE Trans. Magn.*, vol. 32, no. 2, pp. 559–566, Mar. 1996.

[27] W. H. Press, S. A. Teukolsky, W. T. Vetterling, and B. P. Flannery, *Numerical Recipes in C*. Cambridge, U.K.: Cambridge University Press, 2002.

[28] R. E. Knight and T. J. Flack, "Application of domain decomposition and transmission line modelling techniques to 2D, time-domain, finite element problems," *IEEE Trans. Magn.*, vol. 32, no. 2, pp. 559–566, Mar. 1996.

[29] C. Pechstein and B. Juttler, "Monotonicity-preserving interproximation of B-H-curves," *J. Comput. Appl. Math.*, vol. 196, no. 1, pp. 45–57, Nov. 2006.

[30] A. Boglietti, A. Cavagnino, and M. Lazzari, "Modelling of the closed rotor slot effects in the induction motor equivalent circuit," in *Proc. 18th Int. Conf. on Electrical Machines (ICEM 2008)*, 2008, pp. 1–4.

**Babak Asghari** (S'06) received the B.Sc. and M.Sc. degrees in electrical engineering from Sharif University of Technology, Tehran, Iran. Currently, he is a Ph.D. candidate in the Department of Electrical and Computer Engineering at the University of Alberta, Edmonton, AB, Canada. His research interests include real-time digital simulation and control of power systems and electrical drives.

**Venkata Dinavahi** (S'94–M'00–SM'08) received the Ph.D. degree in electrical and computer engineering from the University of Toronto in 2000.

Currently, he is a Professor at the University of Alberta, Edmonton, AB, Canada. His research interests include real-time simulation of power systems and power electronic systems.

READ ONLY